Trends in Physical Chemistry
Vol. 15, 2014

Original Communication

Real-time localization and nanospectroscopy of single epidermal growth factor receptors in live cells

Jung Y. Huang[1,*] and Chien Y. Lin[2]

[1]The T.K.B. Research Center for Photonics, [2]Department of Photonics, Chiao Tung University, Hsinchu, Taiwan 30010, Republic of China.

ABSTRACT

In the present paper, we demonstrate a technique that can simultaneously localize single epidermal growth factor receptors (EGFRs) in live cells and record their spectra as well. This technique has the advantages of both single-molecule sensitivity and parallel detection. By exploiting the environment-induced spectral changes of fluorescently tagged EGFRs, we disclosed that the environments of EGFR dimers in activated cells differ from the environments of EGFRs in cells at rest. This simple approach could open a route for devising a large number of biologically relevant applications that offer the advantages of minimum perturbation and single-molecule parallel detection.

KEYWORDS: single-molecule localization, fluorescence microscopy, EGFR, live cell

1. INTRODUCTION

Many key cellular processes are mediated by a small number of key biomolecules [1]. Conventional methods using organic fluorophores can yield reliable data with mean values from multiple molecular events at a specific time. However, such techniques cannot provide information on how the activities of single molecules fluctuate in different regions of living cells at different times [2, 3]. Following the demonstration by Shera in the 1990s that single molecules of fluorescent dyes could be detected in solutions [4], single-molecule fluorescent imaging and tracking has become a powerful tool to understand the dynamics of cellular organization.

Many biological processes involve varying spatial arrangements of different biomolecules. Multicolor localization of single molecules can yield insight into questions of cellular organization, which have been unanswerable by conventional fluorescence microscopy [5]. In a typical approach of multicolor localization, multiple species are imaged simultaneously by labeling these molecules with fluorophores that have different emission colors. This approach allows for multiplex detection of four different fluorescent species at the most [6]. An improved scheme to probe more molecular species is the use of activator-reporter labeling techniques in which different activator molecules couple to the same reporter molecule. Thereby subsequent imaging of the different channels can be achieved by simply switching the illumination wavelength [7]. To further improve the localization accuracy and enhance signal strength, Mivelle *et al.* recently developed a photonic antenna on the tip of a taped fiber for multicolor imaging of single molecules with nanometer spatial resolution [8]. Impressive performances of 20-nm resolution and 10^3-fold signal enhancement were achieved. However, the technique needs a specially designed scanning near-field probe, which may perturb the dedicated living system under study. For live cell imaging, wide-field multicolor localization offers unique advantages of minimum perturbation and parallel detection. In this regard, several conceptual studies have reported simultaneous measurement of the position and emission color (i.e., the central wavelength

*Corresponding author: jyhuang@faculty.nctu.edu.tw

of a spectrum) of single fluorescent emitters [9, 10, 11]. Broeken *et al.* achieved a wavelength precision of 10 nm and a spatial localization accuracy of 10 nm for 1000 signal photons from fluorescent beads [9]. However, they were unable to demonstrate spectral profile acquisition and single-molecule localization for live cells due to limited emission of single photons from single fluorophores. In this study, we report the simultaneous detection of location and spectrum of fluorescently tagged epidermal growth factor receptors (EGFR) in live cells.

EGFRs and other types of receptors in the plasma membrane are responsible for transducing cellular signals and relaying messages from the external environment to the cellular nucleus [12]. EGFRs contain an extracellular binding domain, a single transmembrane domain, and a cytoplasmic tyrosine kinase domain. Ligands such as epidermal growth factor (EGF) can bind to the extracellular domain and thus stimulate conformational changes in EGFRs that promote receptor dimerization and the activation of the intracellular tyrosine kinase domain [12, 13]. In parallel with experimental evidence for the diffusive motion of receptor proteins, our understanding of the two-dimensional plasma membrane has evolved from a homogeneous environment to a hierarchy of organized structures [14]. How these organized structures of the plasma membrane influence the diffusion properties of receptor proteins in a live cell is a fundamental question in life science. We developed a machine-learning technique to reliably retrieve information from a large number of positions and spectral profiles. By using this method, we disclosed that after EGF-activation in a cell, EGFR molecules appear to move into lipid raft domains and form dimers [15]. Our method successfully captures the dynamic interactions of receptors at the single-molecule level and yields useful information concerning their local cellular environment.

2. EXPERIMENTAL METHODS

2.1. Sample preparation

HeLa cells were cultured in Dulbecco's Modified Eagle's medium with 10% (v/v) fetal bovine serum, but without phenol red. Before the single-molecule live-cell imaging, the cells were plated on a slide with eight-well chambers. After reaching 70-80% confluence, the cells were deprived of serum for 24 h. To visualize EGFR proteins in living cells, we first incubated the live cells with 10 nM anti-EGFR antibody (Thermo Fisher Scientific, Waltham, MA, USA) for 15 min and washed three times with phosphate buffered saline (PBS). The cells were then treated with IgG-Cy3 for 15 min and washed three times again with PBS. The resulting fluorescent EGFR species are denoted as Cy3-ab-EGFR. To activate the cells with epidermal growth factor (EGF), we added 0.1 μg/mL EGF to the cell culture and waited for 10 min before imaging the cells.

2.2. Optical apparatus and spectral calibration

Fig. 1(a) depicts the optical apparatus, which is based on an inverted optical microscope (IX-71, Olympus Optical Co., Tokyo, Japan) equipped with a high numerical aperture oil immersion objective lens. The output from a green (532-nm) solid-state laser was collimated. The L3 lens in Fig. 1(a) focuses the collimated laser beam at the back focal plane of the objective lens to excite fluorescently tagged EGFRs in live cells. The fluorescent signal was filtered with appropriate filters and then detected with an electron-multiplying charge coupled device (EMCCD, Cascade II 512, Photometrics Inc., Huntington Beach, CA, USA). The number of optic devices was minimized in the detection arm to further improve the detection efficiency of single-molecule receptor proteins.

A transmission grating (p = 300 lines/mm) was placed behind the L4 imaging lens. The resulting zero-order diffraction image contains location information and can be used to localize the molecule with a resolution of 30 nm; the first-order image carries the spectral information. To deduce the relationship of wavelength and pixel position, we focused a laser beam onto a sample chamber filled with deionized water. The photons scattered from water were strong enough to clearly form zero and first-order diffraction spots on the EMCCD. Four different laser beams with wavelengths of 405, 473, 532 and 671 nm propagating along the same optical path were applied to the sample. Recorded images are presented in Fig. 1(b). The narrow spectral line width of the lasers allows us to precisely determine the separation distance d between the zero and the first-order diffraction spots. The measured separations and the corresponding wavelengths can be fitted to $w = d \times \tan[\sin^{-1}(-\lambda/p)]$ as shown in Fig. 1(c).

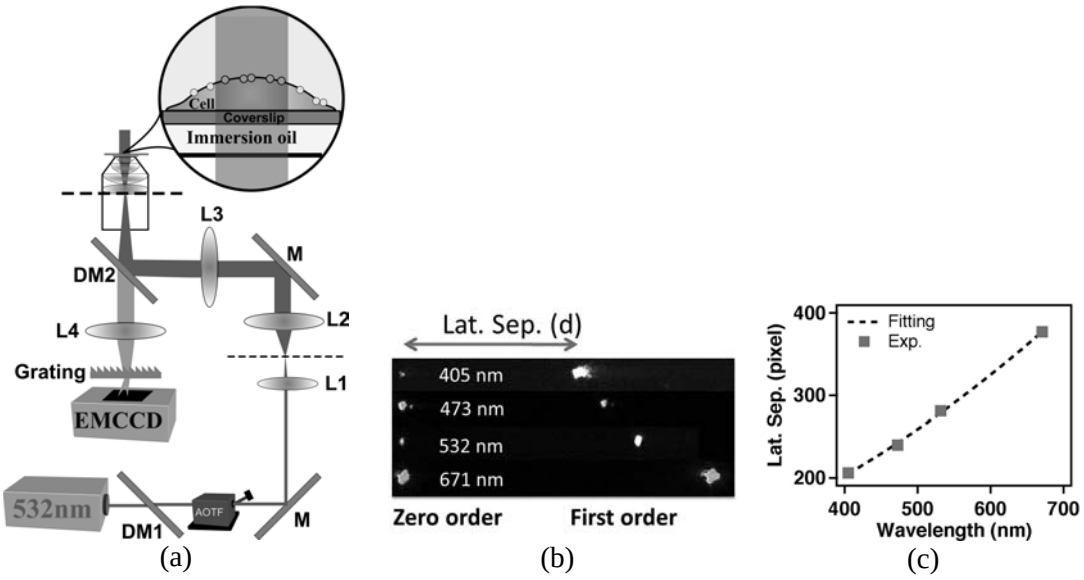

Fig. 1. (a) Experimental setup used to record the location and spectrum of a tagged protein in a living cell. (b) Images of the zero-order and first-order diffraction spots of photons scattered from water at four different wavelengths. (c) The separation between the zero-order and first-order diffraction spots as a function of wavelength.

3. RESULTS AND DISCUSSION

3.1. Real-time localization and nanospectroscopy of fluorescently tagged EGFRs in live cells

Fig. 2(a) presents the zero-order and the first-order diffraction images of Cy3-ab-EGFR in a live HeLa cell. We focused on two Cy3-tagged EGFRs; one located at the position marked by the dotted circle in the zero-order image and the other at the center of the solid circle. Because of the diffraction of fluorescent signal by the grating, the first-order image from the two molecules can exhibit their spectra, which form two lines as indicated in the first-order image, enclosed in the dotted and solid rectangles, respectively. Knowing the position of the fluorophores and the spectral calibration given in Fig. 1(c), we can easily convert each line profile into a spectrum. The resulting spectra of the two Cy3-ab-EGFRs are presented in Fig. 2(b), exhibiting a clear relative shift between the two spectra. The spectral shift can be attributed to the rings of Cy3 fluorophore not lying on the same plane, which results in a nonzero dihedral angle between the two ring planes [16, 17]. The dihedral angle is sensitive to the environment of the Cy3 fluorophores [17]. An increased dihedral angle can reduce the π-conjugation of the molecule and thus perturb the light emitting properties. To confirm that the isolated spots observed in Fig. 2(a) are from single-molecule EGFRs, we fitted the profile of the zero-order spots to a Gaussian distribution to extract the intensity at peak value. The resulting intensity variation versus time falls into two categories: the first one has one-step photo-bleaching (see the short dashed curve in Fig. 2(c)) and the other exhibits two-step photo-bleaching (solid line), thus supporting the conclusion that the spots are emitted by single-molecule EGFR monomers and dimers, respectively.

The EGFR can form homodimers with itself and heterodimers with other members of its receptor-family, such as ErbB-2 [18, 19, 20]. In some cancers, EGFR is overproduced, and that overproduction can alter the equilibrium population of the EGFR species [21]. Thus, it is important to investigate the dimerization of EGFRs in live cells. In this paper, we demonstrate the applicability of our technique on this important topic in real physiological conditions. Simultaneous measurement of the position and emission spectrum of single receptors in live cells is achievable as long as the receptor proteins are tagged with different types of fluorophores that are insensitive to the environment. With the known positions and spectral profiles as input, information on the dynamics of multiple receptors can be revealed even if the receptors spatially overlap. However, the

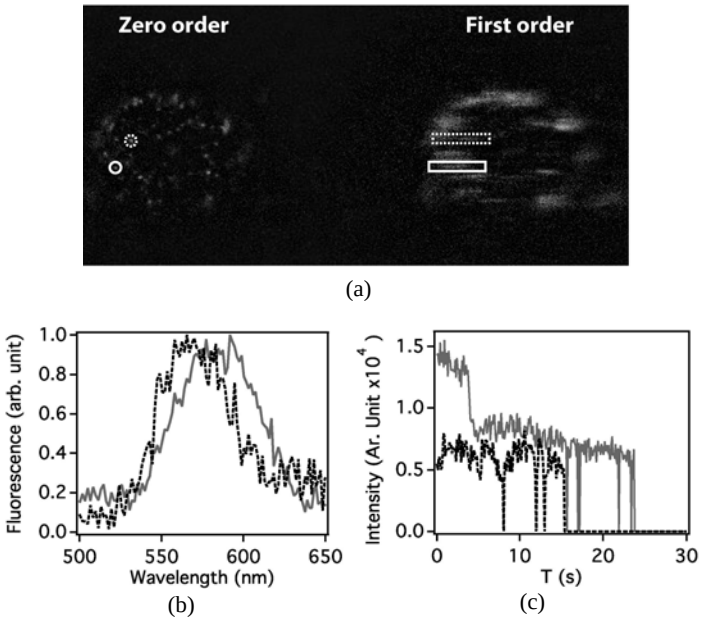

Fig. 2. (a) Zero-order diffraction image and the corresponding first-order image of Cy3-ab-EGFRs in a live HeLa cell. (b) The fluorescent spectra were converted from the line profiles lying inside the solid and dotted rectangles of (a). (c) The intensity variation of the spots versus time clearly exhibits either one-step (short dashed curve) or two-step (solid line) photo-bleaching processes.

situation in our case is more complicated because EGFR proteins in a live cell are labeled with Cy3, which is environment-sensitive. This makes simultaneous retrieval of location and spectrum intractable. To circumvent this difficulty, we collected data from those emitters that were spatially separated for analysis. However, we would like to point out that this limitation can be eliminated by using recently developed super-resolution imaging techniques such as PALM [22], STORM [23], or STED [24].

Fig. 3(a) presents a histogram of fluorescent signals from a large number of Cy3-ab-EGFRs in live HeLa cells before (solid bars) and after (open bars) the cells were activated with EGF. To analyze the data quantitatively, we invoked a self-organizing map algorithm (SOM) to classify the fluorescent intensities [25]. One of the most interesting aspects of a SOM is that it can learn to classify data without supervision. In other word, training a SOM requires no target vector. We can simply command SOM to separate the fluorescent intensities into two classes of monomer and dimer. The SOM will yield a threshold, which is indicated by the vertical line in Fig. 3(a). The threshold optimally separates the monomer intensities from dimers by maximizing the interclass separation while minimizing the total intraclass distance. For the cells at rest, the threshold level locates at 6.5×10^3. For the EGF-activated cells, the threshold was increased by a factor of 2 to about 1.25×10^4 due to activation-induced population change [26, 27]. Student's *t*-test ruled out the null assumption, and supported an intensity distribution consisting of two groups with significance greater than 99%. From the analysis presented in Fig. 3(b), the preformed dimers occupy less than 10% of EGFRs in live HeLa cells at rest. When the cells were activated with EGF, the population of EGFR dimers increased to 45% accompanied by a reduction of monomers from 90% to about 55%. The relative population of the preformed dimers in HeLa cells at rest agrees well with previously reported values [28].

3.2. Classification of spectra

To further deduce information on EGFR environments from the spectra, we reduced a spectral profile into four characteristic parameters: the zero moment (fluorescent intensity), the first moment (central wavelength), the variance (spectral bandwidth), and

the third central moment (left-right asymmetry). A self-organizing map (SOM) provides a way of representing multidimensional data in a lower dimensional space. We can think of the output from a SOM as a feature map of the input space. Therefore, we again applied SOM to classify the set of spectral parameters. By using the SOM machine-learning classifier, we were able to classify the spectra from Cy3-ab-EGFRs into three classes. The first class has an enhanced spectrum on the long wavelength side (marked by green (1) in Fig. 4(a)). The second class possesses an enhanced spectrum on the short wavelength side (marked by blue (2)), and the third one has a red-shifted spectrum (marked by red (3)). Student's t-test ruled out the null assumption, and supported a spectral parameter distribution consisting of three classes with significance greater than 99%.

Cyanine dyes are widely used in biomedical applications. For example, Cy3 can act as a fluorescent molecular rotor for sensing intramolecular

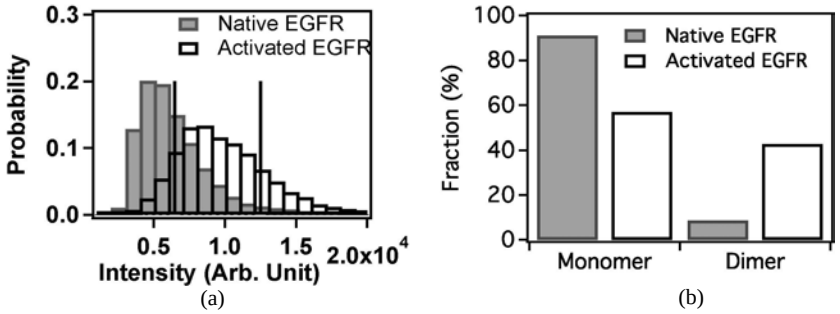

Fig. 3. (a) Histogram of fluorescent intensity from Cy3-ab-EGFR in live HeLa cells, and (b) the deduced population fractions of EGFR monomers and dimers in live HeLa cells before (at rest: filled bars) and after adding EGF (activated: open bars).

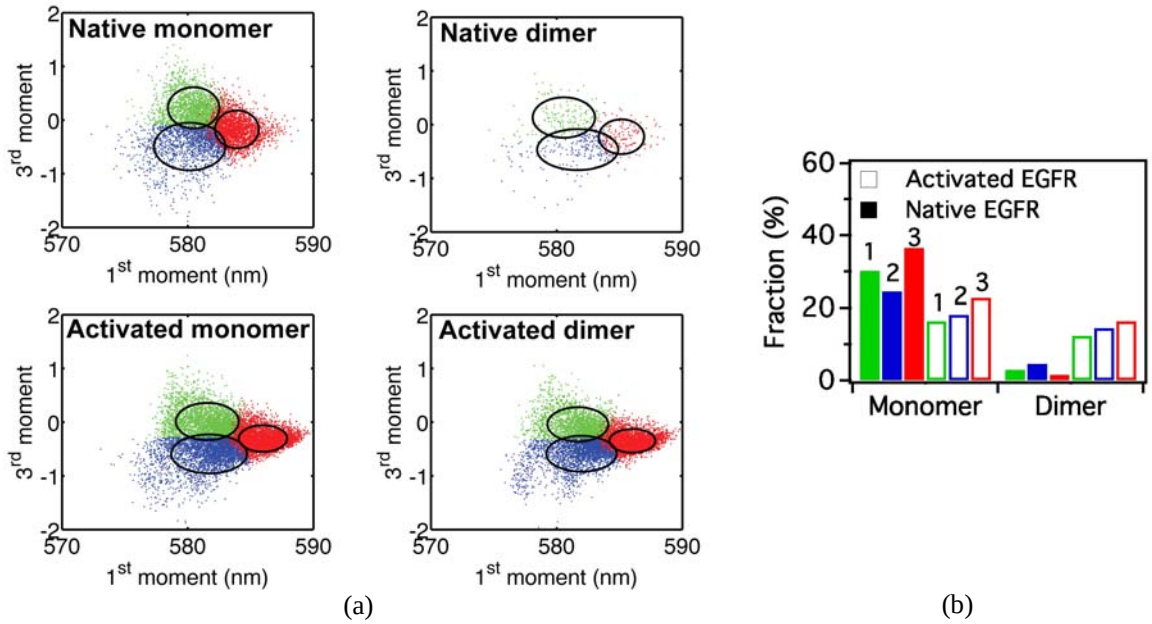

Fig. 4. (a) Correlation plots of the third central moment and the first moment of the spectra of Cy3-ab-EGFRs in live HeLa cells. The ellipses denote the range of 1.5 variances from the centers. (b) The deduced relative population fractions in the three classes for EGFR monomers and dimers in live cells at rest (solid bars: green (1), blue (2), red (3)), and in EGF-activated cells (open bars).

viscosity. The transducing process is based on the mechanism that the viscous environment restricts the internal rotation along the polymethine chain of Cy3 and results in increased fluorescence emission [17]. In our case, each acquired single-molecule spectrum reflects the microenvironmental influence on a Cy3-ab-EGFR. If the Cy3 fluorophore in the plasma membrane of a live cell is stabilized at a specific angle along its polymethine chain, the spectral profile is symmetric and therefore has a vanishing third central moment as represented by the red-colored class in Fig. 4(a). However, if more than one angle is sampled in each exposure time of the EMCCD detector, an asymmetric profile with either a positive or negative third central moment can be produced, yielding the green and blue groups in Fig. 4(a).

Thus, our technique, which allows simultaneous measurements of location and spectrum, can probe into the environmental changes of single receptors in live cells. Fig. 4(b) presents the relative populations of EGFR species before and after activation. The relative populations of EGFR monomers in the green (1), blue (2), and red (3) classes are 33%, 26%, and 40%, respectively in the cells at rest. For the EGFR dimers in cells at rest, the relative populations become 31%, 56%, and 13%. However, in the EGF-activated cells, the relative populations of EGFR complexes in the three classes were found to be similar, with the relative population fractions of 29%, 31%, and 40% for the monomers, and 29%, 33%, and 38% for the dimers. The result suggests that the EGFR monomers and dimers in cells at rest may locate in different environments, whereas by contrast, the environments of EGFR monomers and dimers in activated cells appear to be similar. This finding corroborates our recent investigation [15] that revealed that un-liganded EGFRs at rest are located outside the lipid raft domains. EGF binding causes the receptors to move into the lipid raft domains, resulting in a dimer environment that is similar to that of liganded EGFR monomer in activated cells.

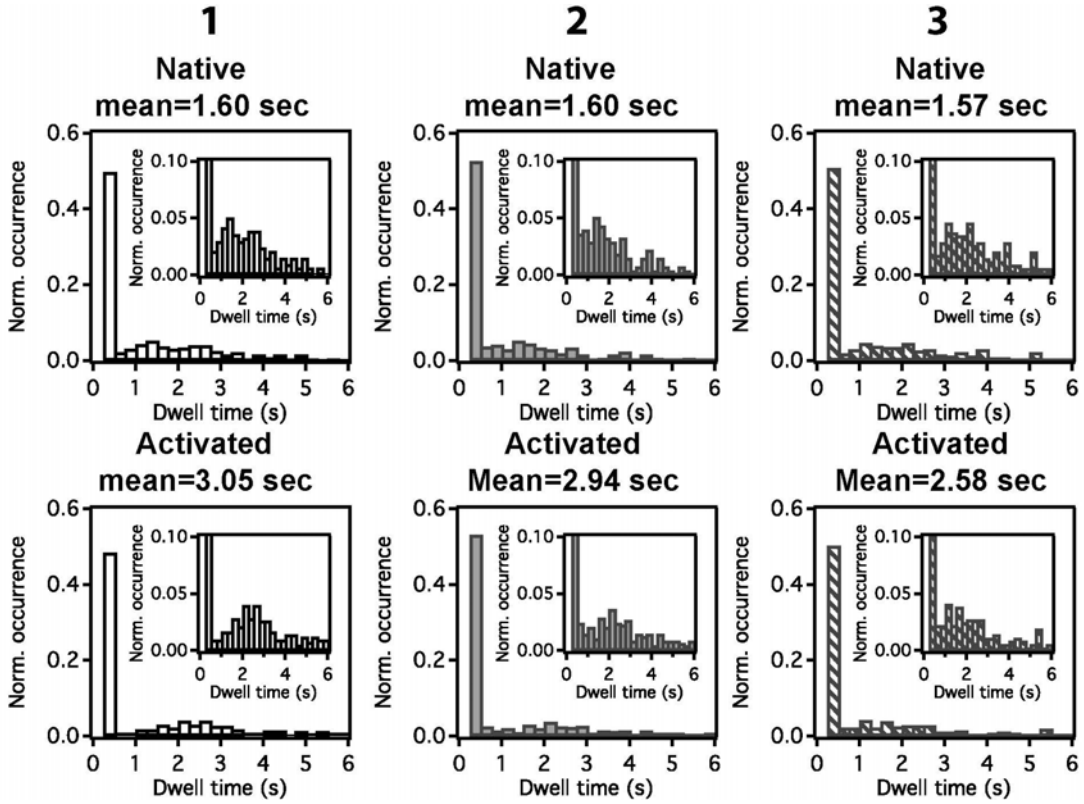

Fig. 5. Histograms of the resident times of EGFR in the three classes (1: green, 2: blue, and 3: red) of Fig. 4. Top row: HeLa cells at rest (native) and bottom row: HeLa cells activated by EGF.

The characteristic parameters presented in Fig. 4(a) were deduced from the spectra, which vary along the trajectories of single Cy3-ab-EGFRs. The dynamical features at different positions of a trajectory can be resolved by dividing the trajectory into several segments with a duration of τ = 100 ms and then extracting the time-resolved parameters from the spectra. From the data, we can further deduce the class-resident times. The results are presented in Fig. 5. We found that the resident times of EGFRs in HeLa cells at rest lie in a range of 1.57-1.60 s. The resident times increased to 2.58-3.05 s after EGF activation, indicating that EGFRs in activated cells diffuse more slowly than that in cells at rest [15, 29]. We can further deduce mean-square displacements (MSD) from the trajectories of Cy3-ab-EGFRs with a time resolution of τ and determine an effective diffusion coefficient with D_{eff} = MSD/(4τ). We found that the effective diffusion coefficient of Cy3-ab-EGFRs decreased by a factor of 4 from 2 $\mu m^2/s$ in the cells at rest to 0.5 $\mu m^2/s$ in the activated cells. We can model the diffusive motion of EGFRs in the plasma membrane as a cylinder with a radius R moving in a medium with viscosity γ. By invoking the Stokes-Einstein relationship $D_{eff} \propto 1/(\gamma R)$, we estimated a decrease in D_{eff} of a factor of 2 from monomer to dimer. EGFR dimers may locate in an environment with larger viscosity, which can reduce the D_{eff} of EGFR dimer to a smaller value than predicted based on the simple geometric effect.

4. CONCLUSION

In summary, we have developed a methodology that can simultaneously measure the location and spectrum of fluorescently tagged proteins in live cells. By exploiting the spectral sensitivity of a probe molecule we can deduce useful information about changes in the environment surrounding the molecule. This technique has both the advantages of single-molecule sensitivity and parallel detection. By using this method, we found that 90% EGFRs of live HeLa cells at rest are in monomer form and less than 10% are in dimer form. After EGF activation, the EGFR dimer population increases to 45%. The fluorescent intensities from Cy3-ab-EGFRs in the live cells can be separated into three classes. The resident times of EGFR monomers in the three classes increase from 1.57-1.60 s in cells at rest to 2.58-3.05 s in activated cells, indicating that EGFRs diffuse more slowly after EGF activation. EGFR monomers and dimers in cells at rest seem to locate in different environments, whereas in activated cells, they appear to locate in a similar lipid domain environment. Our single-molecule optical methodology could open a route for enabling many biological applications that require minimum perturbation and parallel detection.

ACKNOWLEDGEMENTS

JYH would like to thank the National Science Council of the Republic of China for its financial support under grant number MOST 103-2112-M-009-012 -MY3.

CONFLICT OF INTEREST STATEMENT

The authors declare no competing conflicts of interest.

REFERENCES

1. Li, G. W. and Xie, X. S. 2011, Nature, 475, 308.
2. Joo, C., Balci, H., Ishitsuka, Y., Buranachai, C. and Ha, T. 2008, Annu. Rev. Biochem., 77, 51.
3. Weiss, S. 1999, Science, 283, 1676.
4. Shera, E. B., Seitzinger, N. K., Davis, L. M., Keller, R. A. and Soper, S. A. 1990, Chem. Phys. Lett., 174, 553.
5. Pertsinidis, A., Mukherjee, K., Sharma, M., Pang, Z. P., Park, S. R., Zhang, Y., Brunger, A. T., Südhof, T. C. and Chu, S. 2013, Proc. Natl. Acad. Sci. USA, 110, E2812.
6. Testa, I., Wurm, C. A., Medda, R., Rothermel, E., von Middendorf, C., Fölling, J., Jakobs, S., Schönle, A., Hell, S. W. and Eggeling, C. 2010, Biophys. J., 99, 2686.
7. Bates, M., Huang, B., Dempsey, G. T. and Zhuang, X. 2007, Science, 317, 1749.
8. Mivelle, M., van Zanten, T. S. and Garcia-Parajo, M. F. 2014, Nano Lett., 14, 4895.
9. Broeken, J., Rieger, B. and Stallinga, S. 2014, Opt. Lett., 39, 3352.
10. Blab, G. A., Oellerich, S., Schumm, R. and Schmidt, T. 2004, Opt. Lett., 29, 727.
11. Han, R., Zhang, Y., Dong, X., Gai, H. and Yeung, E. S. 2008, Anal. Chim. Acta, 619, 209.
12. Citri, A. and Yarden, Y. 2006, Nat. Rev. Mol. Cell Biol., 7, 505.
13. Lemmon, M. A. and Schlessinger, J. 2010, Cell, 25, 1117.

14. Kusumi, A., Fujiwara, T. K., Morone, N., Yoshida, K. J., Chadda, R., Xie, M., Kasai, R. S. and Suzuki, K. G. 2012, Seminars in Cell and Developmental Biology, 23, 126.
15. Lin, C. Y., Huang, J. Y. and Lo, L. W. 2014, Biochimica et Biophysica Acta, 1848, 886.
16. Cao, J., Wu, T., Hu, C., Liu, T., Sun, W., Fan, J. and Peng, X. 2012, Phys. Chem. Chem. Phys., 14, 13702.
17. Cao, J., Hu, C., Sun, W., Xu, Q., Fan, J., Song, F., Sun, S. and Peng, X. 2014, RSC Adv., 4, 13385.
18. Lemmon, M. A. and Schlessinger, J. 2010, Cell, 25, 1117.
19. Lemmon, M. A. 2009, Exp. Cell Res., 315, 638.
20. Szabo, A., Szollosi, J. and Nagy, P. 2010, Biophys. J., 99, 105.
21. Arteaga, C. L. and Engelman, J. A. 2014, Cancer Cell, 25, 282.
22. Eric Betzig, E., Patterson, G. H., Sougrat, R., Lindwasser, O. W., Olenych, S., Bonifacino, J. S., Davidson, M. W., Lippincott-Schwartz, J. and Hess, H. F. 2006, Science, 313, 1642.
23. Huang, B., Bates, M. and Zhuang, X. 2009, Annual Review of Biochemistry, 78, 993.
24. Westphal, V., Rizzoli, S. O., Lauterbach, M. A., Kamin, D., Jahn, R. and Hell, S. W. 2008, Science, 320, 246.
25. See the url http://www.ai-junkie.com/ann/som/som1.html
26. Sako, Y., Minoghchi, S. and Yanagida, T. 2000, Nature Cell Biol., 2, 168.
27. Kawashima, N., Nakayama, K., Itoh, K., Itoh, T., Ishikawa, M. and Biju, V. 2010, Chem. Eur. J., 16, 1186.
28. Morikia, T., Maruyamaa, H. and Maruyama, I. N. 2001, J. Mol. Bio., 311, 1011.
29. Chung, I., Akita, R., Vandlen R., Toomre, D., Schlessinger, J. and Mellman, I. 2010, Nature, 464, 783.